IOP Conf. Series: Materials Science and Engineering **139** (2016) 012021 doi:10.1088/1757-899X/139/1/012021

Use of micro-tomography for validation of method to identify interfacial shear strength from tensile tests of short regenerated cellulose fibre composites

A Hajlane[1], A Miettinen[2], B Madsen[3], J Beauson[3] and R Joffe[1]

[1]Luleå University of Technology, Department of Engineering Sciences and Mathematics, SE-971 87 Luleå, Sweden
[2]University of Jyvaskyla, Department of Physics, P.O. Box 35 (YFL) FI-40014 Jyvaskyla, Finland
[3]Technical University of Denmark, Department of Wind Energy, Risø Campus, Frederiksborgvej 399, 4000 Roskilde, Denmark

e-mail: Roberts.Joffe@ltu.se

Abstract. The interfacial shear strength of short regenerated cellulose fibre/polylactide composites was characterized by means of an industry-friendly adhesion test method. The interfacial shear strength was back-calculated from the experimental tensile stress-strain curves of composites by using a micro-mechanical model. The parameters characterizing the micro-structure of the composites, e.g. fibre length and orientation distributions, used as input in the model were obtained by micro-tomography. The investigation was carried out on composites with untreated and surface treated fibres with various fibre weight contents (5wt%, 10wt%, and 15wt% for untreated fibres, and 15wt% for treated fibres). The properties of fibres were measured by an automated single fibre tensile test method. Based on these results, the efficiency of the fibre treatment to improve fibre/matrix adhesion is evaluated, and the applicability of the method to measure the interfacial shear strength is discussed. The results are compared with data from previous work, and with other results from the literature.

1. Introduction

During recent years, cellulosic fibres (natural and manmade) have been considered as feasible replacement of synthetic reinforcement (e.g. glass fibres) for polymer composites designed for long term use in structures. The driving force for such development is the concern regarding impact of production of composites on environment, and the growing demand for sustainable and recyclable materials. This trend is also reflected in the growing number of publications on the subject as shown in literature reviews [1-2] on development of bio-based engineering materials.

One of the weaknesses of cellulosic fibres is their typical poor compatibility with polymers, and the resulting weak fibre/matrix adhesion which strongly affects the mechanical properties of composite materials. This problem can be addressed by modifying the fibre surface to enhance the chemical bonding between composite constituents [3]. The problem can also be addressed by creating hierarchical reinforcement (combining nano- and micro- scales) with larger surface area to promote both, chemical and mechanical, fibre/matrix interaction. Hierarchical reinforcement can be created by grafting of nano-size particles on micro-size fibres, and this is believed to enhance the fibre/matrix adhesion. For example, it has been shown that the grafting of carbon nano-tubes on conventional

fibres increases the through thickness performance of composites due to strengthening of fibre/matrix adhesion by improving the fibre surface area, and by creating mechanical interlocking [4]. In another example, composites based on hierarchical cellulosic fibres were successfully achieved by depositing bacterial cellulose on natural fibres [5]. The tensile and flexural properties of the composites of hierarchical sisal fibres embedded in acrylated epoxidised soybean oil resin were significantly improved over neat fibre reinforced composites. In the current study, cellulose nano-whiskers extracted from date palm trees are deposited onto regenerated cellulose fibres.

One of the important parts of the optimization process of the fibre/matrix interface is its characterization to evaluate the efficiency of various fibre treatment methods. The usual way to characterize the fibre/matrix adhesion is by determining the interfacial shear strength (IFSS). There is number of direct and indirect methods to evaluate IFSS, ranging from tests on single fibres (fibre pull-out, micro-droplet test, single fibre fragmentation) to test on full scale composites (e.g. short beam shear). However, these methods, especially those on micro-scale, are time consuming and not easy to perform, and moreover the results may significantly vary between different methods. Therefore, there is a need for a simple, fast, and yet reliable technique to measure IFSS in composites. The method used in the present study has been considered to be the most industry-friendly one [6], and is a modification of a method originally presented in [7-8]. The model scheme is based on analysis of the tensile stress-strain curves of a composite system. Two different strain values are used to obtain values for IFSS and the fibre orientation factor.

The current study follows the method presented in [6-8]. All experimental parameters related to the composite morphology and fibre properties are obtained directly from experiments. This allow more reliable predictions by the micro-mechanical models since input parameters are accurately measured rather than estimated based on materials datasheets and assumptions. The output of the approach proposed in [6-8] is compared with the results obtained based on X-ray tomography data, and possible factors responsible for discrepancies between methods are discussed.

2. Theoretical background

Based on the Kelly-Tyson model for the strength of aligned short fibre composites [9], and by dividing the total fibre volume fraction (V_f) into sub-fractions of fibres with given lengths (L_f), Bowyer and Bader [7] developed a model to predict stress (σ_c) as function of strain (ε_c) in composites with non-aligned fibres:

$$\sigma_c = \eta_o \left(\sum_i \left[\frac{\tau_i \, L_{f(i)} \, V_{f(i)}}{d_f} \right] + \sum_j \left[E_f \, \varepsilon_c \, V_{f(j)} \left(1 - \frac{E_f \, \varepsilon_c \, d_f}{4 \, \tau_i \, L_{f(j)}} \right) \right] \right) + (1 - V_f) \, E_m \, \varepsilon_c \qquad (1)$$

where η_o is the fibre orientation factor, d_f is the fibre diameter, E_f is the fibre stiffness, and τ_i is the interfacial shear strength.

It is assumed that a critical fibre length ($L_{f\,crit\,(\varepsilon)}$) is defined for any given strain level:

$$L_{f\,crit\,(\varepsilon)} = \frac{E_f \, \varepsilon_c \, d_f}{2 \, \tau_i} \qquad (2)$$

Fibres shorter than $L_{f\,crit\,(\varepsilon)}$ contribute with the index i in equation (1), and fibres longer than $L_{f\,crit\,(\varepsilon)}$ contribute with the index j in equation (1).

By selecting two strain levels from a measured stress-strain curve of a given composite system, and by following the described fitting approach in Bowyer and Bader [7], a single value for τ_i (IFSS) and a single value for η_o can be determined.

It should be noted that the term $E_f \cdot \varepsilon_c$ in equations (1) and (2) corresponds to the fibre stress (σ_f). Likewise, the term $E_m \cdot \varepsilon_c$ in equation (1) corresponds to the matrix stress (σ_m). This is assuming linear stress-strain behaviour of fibres and matrix. If stress-strain curves are measured for fibres and matrix, the accurate stress levels (σ_f and σ_m), at a given composite strain level, can be used in the equations.

3. Experimental

This section very briefly presents experimental details about the surface treatment of fibres, manufacturing of composites as well as characterization of fibre and composite properties, including detailed characteristics of the internal structure of the composite materials. More complete information concerning the applied procedures can be found in [10-13].

3.1. Materials

The regenerated cellulose fibre (RCF) Cordenka 700 Super 3, 2440 dtex, Z100 (Z100 refers to twist, 100 rev/meter) was used as received. Fibres were supplied in the form of bundles, each bundle contains 1350 fibres and average diameter of single fibre is 12.5 microns (assuming circular cross-section). Density of fibres is 1.50 g/cm^3.

For the modification of the fibre surface, a number of different chemicals were used. The initiator cerium ammonium nitrate (CAN), nitric acid, NaOH, MPS (organo-functional trialkoxy silane γ-methacryloxypropyl trimethoxysilane) and pure ethanol (99%) were used as received without purification. Distilled water was employed as co-solvent with ethanol for the grafting reaction. Cellulose nano-whiskers (CW) were extracted from date palm tree according to the procedure reported in [11].

Polylactic acid (PLA) biopolymer was used as matrix in composites. The polymer specification is Ingeo biopolymer 2003D from NatureWorks LLC. Density of PLA is 1.24 g/cm^3.

3.2. Fibre surface treatment

The fibre treatment was carried out in two steps. First a silane treatment of fibres was performed and then CW were grafted onto the RCF surface (see [12] for details).

The silane treatment was performed as follows: a 1600 ml mixture of ethanol and water (50/50 v%) was poured into a reactor and heated up to 65°C; after stabilizing the temperature, NaOH and nitric acid solutions were utilized to adjust pH to 7; once pH was stabilized (after approximately 2 hours), 16 grams of fibres, wound on a holder and fixed on a mechanical stirrer, were introduced into the solution (the ratio of fibres and solvent was adjusted to be 1% w/v); the polymerisation (or co-polymerisation) of MPS was carried out by adding first CAN 10^{-3} mol/L in the reactor and then stirring for 30 minutes. Meanwhile, the mixture was purged with nitrogen gas for 15 minutes to remove any dissolved oxygen gas. At this stage, free radicals are supposed to be created at the surface of the cellulose backbone, and are ready to react with vinyl monomers (MPS). To initiate the graft co-polymerisation, 10^{-3} ml/L of MPS was added to the reactor, and the nitrogen gas flow was maintained until the end of the reaction (5 hours) while stirring at medium constant rate. Fibres were then washed two times in ethanol and once in water to remove unreacted products and other impurities trapped in the fibres.

The grafting process of the nano-whiskers was performed by using CW in a 0.2 wt% concentration. Distilled water (1600 ml) was poured in the reactor and pH was adjusted to be between 4 and 5. When pH was stabilized, the MPS-modified fibres were re-placed in the reactor. Prior to sonication, a solution of NaOH (0.1 M) was added to the cellulose nano-whiskers to reduce the amount of sulfonate groups and release the hydroxyl (or alcoholate) groups of CW. The CW suspension was then sonicated for 5 minutes and added into the reactor.

The reaction was maintained at medium stirring rate at room temperature for 5 hours. Afterwards, the fibres were washed three times in distilled water and dried at 110°C for 4 hours under vacuum.

Finally, the treated fibres were stored in a desiccator to protect the fibres from dust.

3.3. Manufacturing of short fibre composites

In order to manufacture short fibre composites with randomly oriented fibres, the continuous RCF were cut to produce 2 mm long bundles. The cutting was done by using an array of 60 razor blades (see [10] for details).

The manufacturing of composite specimens consisted of two stages: 1) homogenization of RCF fibres and PLA granules to produce composite pellets; 2) injection moulding of test specimens. The homogenization of fibres and PLA was carried out in a twin-screw Brabender PLE 650 mixer. The mixing was done for 5 minutes at 215°C with screw rotation of 70 rpm. Directly after mixing, the material was pressed into flat 2 mm thick plates in a hydraulic manually operated press preheated to 80°C. The plates were cut into small pieces to produce composite pellets with a square shape (approximately 2-3 mm in size). Composite pellets were fed into a HAAKE™ MiniJet laboratory injection moulding machine (Thermo Scientific™, Karlsruhe, Germany) to produce tensile specimens according to ASTM D638 (type 5 dog-bone specimens). Detailed information about the manufacturing procedure and conditions can be found in [10].

Four different composite compositions were produced (six specimens for each): three composites of PLA with untreated fibres (5, 10 and 15 wt%), and one composite of PLA with treated fibres (15 wt%).

3.4. Characterization of fibres

In order to evaluate if the fibres are degraded during the composite manufacturing process, fibre bundles were thermally conditioned to simulate the applied composite processing conditions (exposure to 220°C for 15 min). Accordingly, in total, four types of fibres were characterized: 1) untreated and unconditioned (U-UC); 2) untreated and conditioned (U-C); 3) treated and unconditioned (T-UC); 4) treated and conditioned (T-C).

Tensile tests of single fibres were carried out using a Textechno machine (Favimat and Airobot2). The linear density of fibres was obtained by a vibroscopy test. The cross-sectional area of fibres was calculated from its linear density, and the density of cellulose (1.50 g/cm^3). In total 50 fibres of each type were tested with gauge length of 50 mm. Tests were carried out in displacement controlled mode with a speed of 5 mm/min.

3.5. Tensile tests of composites

Tensile tests of composites were carried out on an Instron 3366 electro-mechanical testing machine equipped with a 10 kN load cell and pneumatic grips. Displacement controlled mode was used with a strain rate set to approximately 1 %/min. An Instron 2620-601 extensometer with a gauge length of 12.5 mm was used to register strain. All experiments were carried out at ambient laboratory conditions (T ~ 24°C, RH ~ 42%) without prior conditioning of specimens. At least four samples for each type of composite were tested. A more detailed description of the procedure is presented in [10].

3.6. X-ray micro-tomography

X-ray micro-tomography was used to determine the fibre length and orientation distribution in the composites while the fibre orientation factor is calculated according to Krenchel's model [14]. First, cylindrical samples of approximately 2 mm in diameter were cut from the central part of tensile test specimens of each of the four composite types. The samples were imaged using Xradia MicroCT-400 tomograph with 1.2 µm pixel size, 30 kV acceleration voltage and 3 W X-ray tube power. After reconstruction, the images were filtered with Gaussian blur (standard deviation = 1 pixel) and thresholded, yielding a binary image of fibres. The threshold value was chosen such that the average fibre diameter was 12.5 µm. Regions whose volume was less than 500 pixels were removed from analysis as they were primarily caused by imaging noise. Fibre diameter, fibre length, fibre orientation distribution as well as fibre orientation factor were then determined as described in [13].

4. Results and discussion

This section consists of two parts; first experimental data are reported and discussed, and then the outcome of processing of results is presented with assessment of applicability of models as well as comparison with other available data.

4.1. Experimental results

The typical stress-strain curves for untreated and treated conditioned fibres are presented in figure 1 (left). It is evident that the performance of the fibres is drastically affected by the treatment and conditioning. This is also shown by the analysis of fibre strength distribution as shown in figure 2 (left) by plotting probability of failure P_f as a function of stress at failure σ. The strength distribution was analysed by fitting a Weibull two-parameter statistical distribution to the experimental data (the same procedure as described in [15] is used). The parameters of the distribution (scale σ_0 and shape m) are shown in figure 2 (right). The summary of average fibre properties (diameter, stiffness, strength) along with Weibull parameters are presented in table 1. The results for unconditioned untreated fibres are in line with previously reported results for similar RCF [16-17]. The results in table 1 show that treatment reduces fibre stiffness by 5% and strength by approximately 25%. The thermal conditioning does not affect stiffness of untreated fibres and reduces it for treated fibres by about 7%. However, strength is much more affected by thermal conditioning, it is reduced by 16% for untreated fibres and by 63% for treated fibres. It also should be noted that scatter of strength has significantly increased for treated conditioned fibres (the shape parameter is much lower than for all other fibres). Since during the manufacturing of composites, fibres are subjected to the same temperatures as during the thermal conditioning, it is assumed that it has the same effect on fibre performance in composites. Therefore, in all further calculations, properties of conditioned fibres were used.

The typical stress-strain curves for unreinforced PLA and the four different composites are shown in figure 1 (right). The average mechanical properties of composites are summarized in table 2. The results show that stiffness and maximum stress increases with increase of fibre content in the composites. The performance of composites with 15wt% of treated RCF is lower than that for untreated RCF composites, which is expected since fibre performance was degraded by treatment and thermal conditioning (see table 1). It should be noted that for all of the composites with untreated fibres and for unreinforced PLA, the strain at maximum stress is almost the same (between 2.6% and 2.8%). The results on mechanical performance presented here compare very well to the data for RCF/PLA composites reported in [18] (although fibre length and orientation in that study may differ).

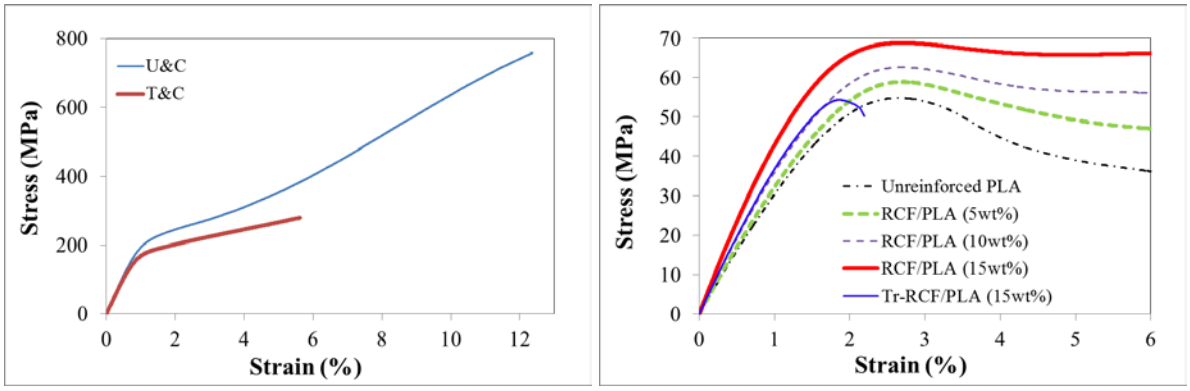

Figure 1. Typical stress-strain curves from single fibre tensile tests of untreated and treated conditioned fibres (left). Typical tensile stress-strain curves for unreinforced polymer and short fibre composites with untreated and treated fibres (right).

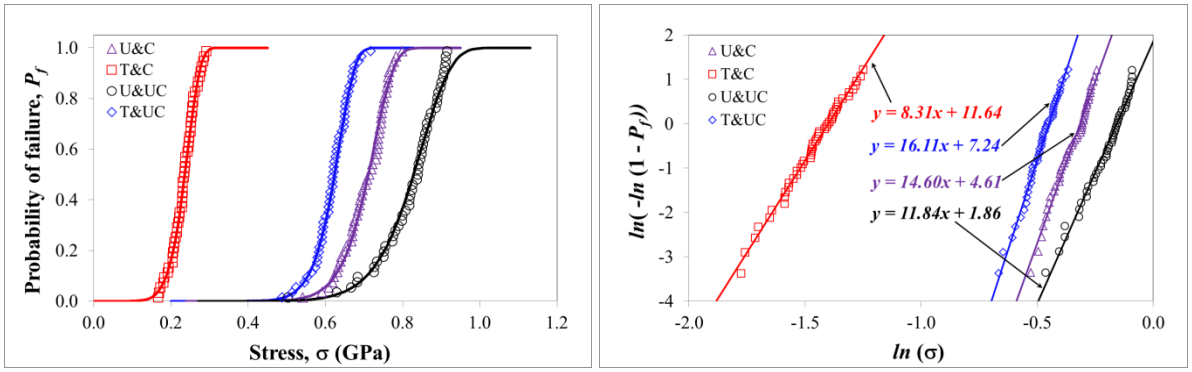

Figure 2. Fibre strength distribution obtained from single fibre tensile tests (symbols in the left plot) and determination of parameters of Weibull distribution (plot on the right). The theoretical Weibull strength distributions are shown as solid lines in the plot on the left.

Table 1. Single fibre tensile test results and parameters of Weibull distributions.

Batch	Fibres	d_f [μm]	Strength [GPa]	Stiffness [GPa]	Shape parameter m	Scale parameter σ_0 [GPa]	$<\sigma>^a$ [GPa]
U-UC	Untreated Unconditioned	12.4 ± 0.2	0.82 ± 0.08	24.04 ± 0.39	11.84	0.86	0.82
U-C	Untreated Conditioned	12.4 ± 0.2	0.69 ± 0.08	23.87 ± 0.45	14.60	0.73	0.70
T-UC	Treated Unconditioned	12.4 ± 0.3	0.62 ± 0.05	22.89 ± 0.45	16.11	0.64	0.62
T-C	Treated Conditioned	12.5 ± 0.2	0.23 ± 0.03	21.50 ± 0.52	8.31	0.25	0.23

[a]Average fibre strength calculated by using parameters of Weibull distribution.

Table 2. Average mechanical properties of neat PLA and RCF reinforced composites.

Batch	Stiffness[a] [GPa]	Max stress [MPa]	Strain at max stress [%]
PLA	3.30 ± 0.13	54.2 ± 0.8	2.64 ± 0.12
RCF/PLA 5wt%	3.52 ± 0.20	57.7 ± 1.4	2.68 ± 0.15
RCF/PLA 10wt%	3.91 ± 0.19	63.9 ± 0.9	2.78 ± 0.15
RCF/PLA 15wt%	4.78 ± 0.13	70.2 ± 1.8	2.66 ± 0.06
Tr-RCF/PLA 15wt%	4.07 ± 0.19	52.5 ± 2.4	1.76 ± 0.10

[a]Measured within strain interval of 0.05%-0.25%.

The determined fibre length and orientation distributions are presented in figure 3 and figure 4, respectively. The results in figure 3 show that fibres were rather significantly reduced in length during the injection moulding process. Initially the fibre bundles were manually cut to 2 mm long pieces, and the final fibre length in the composites is within interval of 0 mm – 1 mm with majority of fibres being around 0.1 mm – 0.3 mm long.

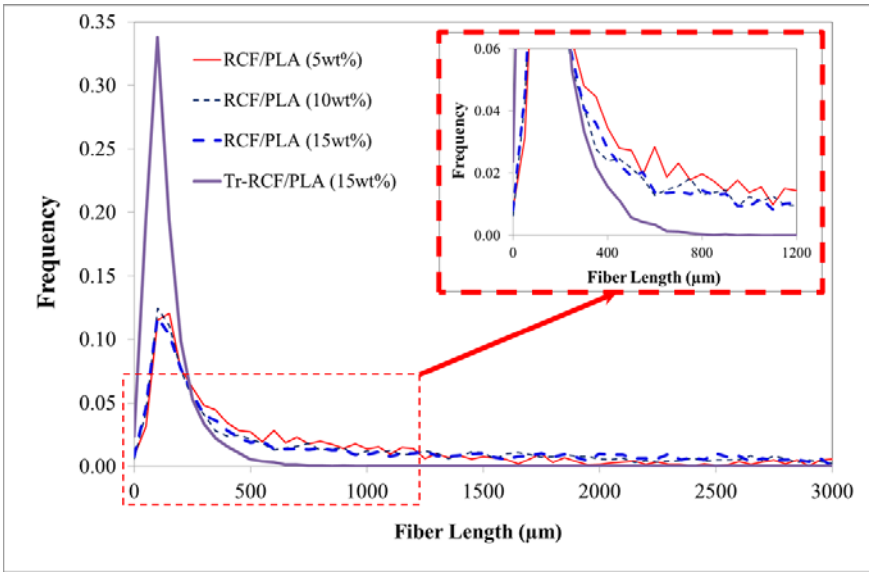

Figure 3. Fibre length distribution obtained from X-ray tomography of composites.

Table 3 summarizes results of the X-ray tomography. It is clear from those data that all untreated fibres have very similar average fibre length (in range 0.266 mm – 0.280 mm) independent of fibre content in the composites, while treated fibres are more than two times shorter. This can be explained by much lower mechanical properties of the treated fibres due to the severe thermal degradation which makes it much easier to break up fibres during composite manufacturing.

The fibre orientation distribution in figure 4 show that fibres are not completely randomly oriented and there is some fibre alignment towards the loading direction (majority of fibres are oriented within 0º-45º with respect to the loading direction). However, the alignment with loading direction is not dominant. It is also worth noticing that treated fibres are less oriented than untreated fibres, which is likely related to their length being shorter.

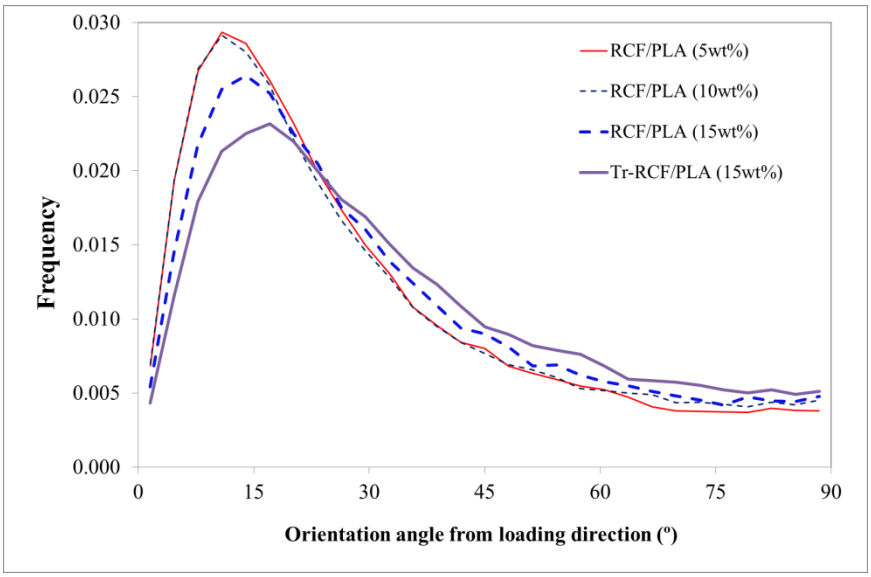

Figure 4. Distribution of angles between fibre direction and loading direction, obtained from X-ray tomography of composites.

The volume fraction of fibres in the composites measured from X-ray tomography agree very well with the values obtained by converting fibre weight fractions into volume fraction by using the density of constituents. Only for composites with 5wt% untreated fibres and 15wt% untreated fibres there is some discrepancy which can be explained by the small volume of composite that is scanned during the X-ray tomography (the fibre distribution may slightly vary along the specimen). Such a good correspondence between measured and theoretically calculated fibre volume fractions indicates that the composites are almost void free. This can be also seen from the images of composite cross-sections obtained from X-ray tomography (see figure 5). In order to avoid error due to the localized measurements, the theoretical fibre volume fractions are used in the further calculations. Inspection of the images in figure 5 also suggests that the fibres are evenly dispersed in the composites.

The fibre orientation factor is also very similar for all composites, being slightly lower for the composite with treated RCF. 3D X-ray tomography images showing fibres in composites are presented in figure 6. Altogether, the data in table 3 and in figures 4 and 6, show that the orientation of fibres is not completely random (orientation factor is higher than that for randomly oriented fibres ~0.4) but it is not clearly unidirectional either (the orientation factor is much smaller than 1).

Table 3. Fibre geometry and content (average values) obtained from X-ray tomography of composites.

Composite	Fibre length L [μm]	Aspect ratio L/d_f	Orientation factor η_o	Fibre volume fraction V_f [%]	Fibre volume fraction, theory[a] V_f^{th} [%]
RCF/PLA 5 wt%	266	21.3	0.62	5.2	4.2
RCF/PLA 10 wt%	281	22.5	0.61	8.6	8.4
RCF/PLA 15 wt%	277	22.1	0.57	12.8	12.7
Tr-RCF/PLA 15 wt%	123	9.9	0.53	11.5	12.7

[a]Calculated from fibre weight fraction and densities of constituents.

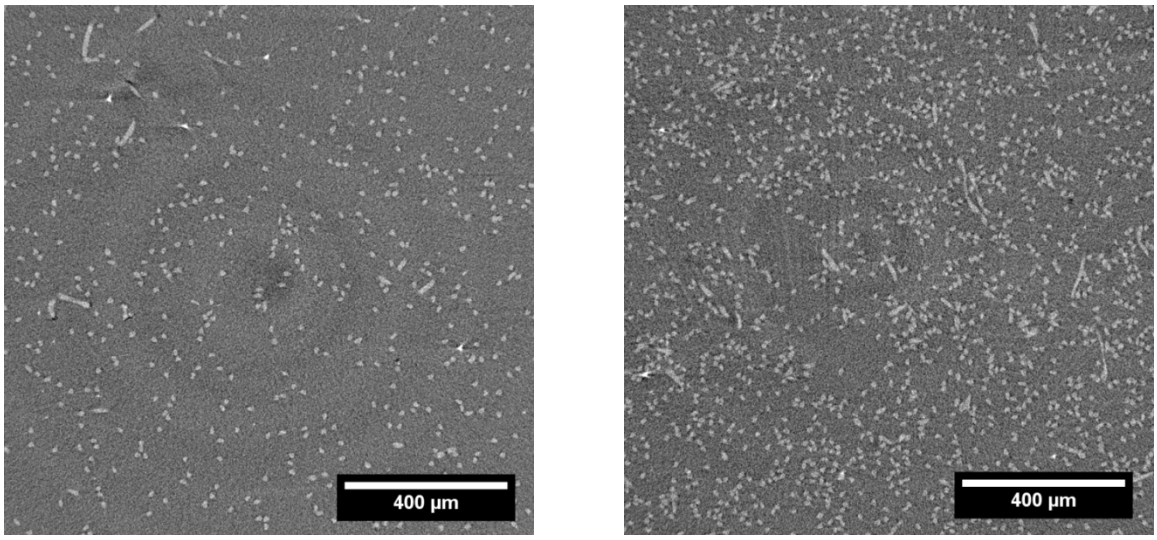

Figure 5. Cross-sections of 5%wt (left) and 15%wt (right) composites obtained from X-ray tomography. The discrete bright regions are cross-sections of individual fibres and the continuous grey region is matrix.

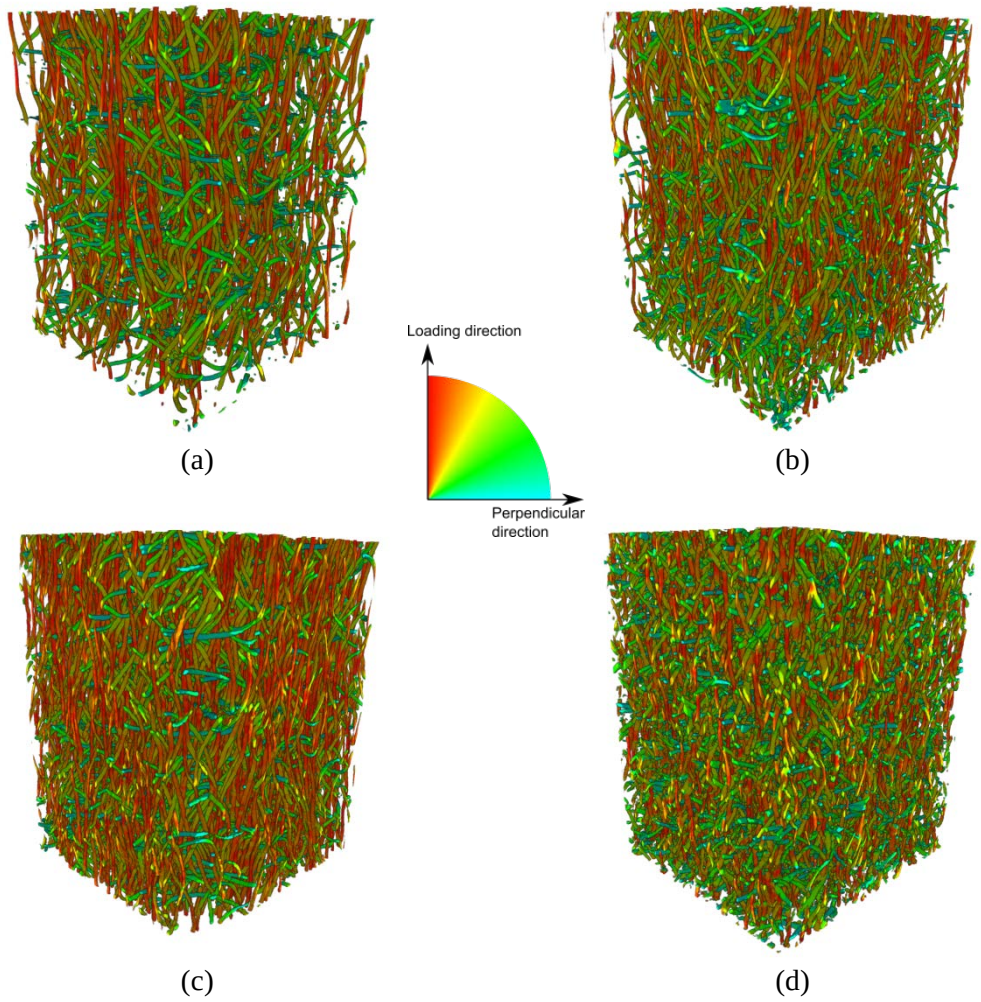

Figure 6. 3D X-ray tomography images of fibres in composites visualizing fibre orientation with colour coding: RCF/PLA (5wt% (a), 10wt% (b), 15wt% (c)) and Tr-RCF/PLA 15wt% (d).

4.2. Calculation of IFSS

The calculation of the IFSS was carried out in a couple different ways by the following procedures:

a) According to method proposed in [6], using two data points from stress-strain curves of composites (figure 1, right) and fitting IFSS and fibre orientation factor according to equations (1) - (2). A linear-elastic behaviour of reinforcement is assumed (using fibre stiffness from table 1 for conditioned fibres). For PLA matrix, the experimental stress-strain curve is used.
b) According to method proposed in [6], but only IFSS is fitted. The fibre orientation factor obtained from X-ray tomography is used (see table 3).
c) The whole stress-strain curve of composites up to the maximum stress value is fitted by the least squares method to obtain IFSS. This approach has been successfully applied to cellulosic fibre composites in [19-20]. The fibre orientation factor from X-ray tomography is used also in this case.

The results of the calculations of IFSS are summarized in table 4, the notation for methods are used according to the list presented above. The data obtained by fitting both IFSS and the fibre orientation factor (method a), show that IFSS is decreasing as the fibre volume fraction is increasing, while the orientation factor is increasing (only untreated fibres are compared). While values for 5wt% and 10wt% are comparable (approximately 15% difference), the biggest change is observed for the composite with 15wt% of fibres. A detailed discussion on such phenomena can be found in [19-20],

where it is suggested that friction induced by residual thermal stresses may affect the measured IFSS, and since residual stress is affected by fibre content in the composite so is the measured IFSS. However, even though changes of IFSS (increase or decrease) with fibre content have been observed in short fibre composites, the changes for 15wt% are too dramatic (approximately 3 times compared to 5wt% and 10wt% composites) to be attributed to the frictional forces. Moreover, the fitted value of the fibre orientation factor for the 15wt% composite is very close to 1, which corresponds to perfect fibre alignment, and this is obviously not the case as shown by X-ray tomography (see table 3, and figures 4 and 6). The fibre orientation factors for 5wt% and 10wt% composites are lower than the values obtained from X-ray tomography (by about 20% – 40%), nevertheless these values seem to be more reasonable than the one obtained from fitting for the 15wt% composite. It should be noted that the orientation factor for the 15wt% composite with treated fibres is very close (but lower) to the value from X-ray tomography (only 8% difference).

The results obtained from methods (b) and (c) show a different trend with respect to IFSS than method (a), IFSS is increasing with fibre content (composites with untreated fibres are compared). However, also in this case, values of IFSS obtained from 5wt% and 10wt% composites are fairly comparable (25% - 33% difference), while the value calculated for the 15wt% composite is much higher (2-3 times). Although the IFSS values obtained in this study by the different methods vary rather significantly, it should be noted that the results obtained for the PLA/Cordenka composite system are similar to the IFSS reported in the literature for other cellulosic fibre composite systems. For example, IFSS obtained for Lyocell/PLA from fibre pull-out test [21] is 10.3-12.0 MPa (depending on fibre treatment), for flax/PLAA obtained from microbond, it is 9.9-22.2 MPa [22] (depending on thermal treatment of fibres), and for flax/PLGA, hemp/PLGA, and sisal/PLGA, it is 9.0 MPa, 11.3 MPa, and 14.3 MPa, respectively [23].

Table 4. Summary of the calculations of IFSS and the fibre orientation factor by different methods.

Material	RCF/PLA 5wt%		RCF/PLA 10wt%		RCF/PLA 15wt%		Tr-RCF/PLA 15wt%	
Method	IFSS [MPa]	η_o	IFSS [MPa]	η_o	IFSS [MPa]	η_o	IFSS [MPa]	η_o
a	14.1	0.39	12.2	0.50	4.5	0.93	25.7	0.49
b	4.7	0.62[a]	7.0	0.61[a]	17.7	0.57[a]	19.7	0.53[a]
c	5.0	0.62[a]	6.7	0.61[a]	12.9	0.57[a]	17.6	0.53[a]

[a]From X-ray tomography.

Even though reliability of the obtained IFSS values may be questioned, it is worth noticing that independently on the method used to calculate IFSS, the values obtained for treated fibres are consistently higher than those for untreated fibres. This may indicate that the chemical treatment of the fibres does improve adhesion between RFC and PLA.

As it was shown above (see figure 1), the stress-strain curves of the Cordenka RCF are highly non-linear, and the composites based on these fibres also exhibit non-linear stress-strain behaviour. Thus, it would be logical to use actual stress-strain curve for fibres rather than the assumed linear-elastic behaviour in the calculation procedure of IFSS. This approach was tried out in this study but the values of IFSS obtained from these try-outs were unreasonably high, or it was not possible at all to fit stress-strain curves for composites by the least square method. Therefore, these results are not presented and discussed in this paper, since no reasonable conclusive explanation of this problem has been found yet. Only speculations regarding possible reasons for discrepancy between modelling and experimental results may be offered at this point. It may be possible that the proposed model in [6-8] is not applicable for composite materials which exhibit highly non-linear behaviour (with viscoelastic and viscoplastic phenomena). It is also possible that the use of only axial fibre stiffness in the model is not sufficient, since RFC is expected to show anisotropic properties. Further investigation of abovementioned factors should be carried out in order to develop more appropriate and stable procedure for the characterization of composites containing highly non-linear reinforcement.

5. Conclusions

A comprehensive characterization of regenerated cellulose fibres and their composites based on a PLA matrix was carried out in order to evaluate interfacial shear strength in the composites. The internal structure of composite was characterized by X-ray tomography, and input parameters (e.g. fibre length and orientation distributions) for micro-mechanical models were obtained. The stress-strain curves of short fibre composites with different fibre volume fractions were used to calculate the interfacial shear strength. The obtained results are comparable to the data reported in the literature acquired from other direct test methods (e.g. fibre pull-out or microbond techniques).

The results obtained in this study, however, are somewhat unreliable and depend very much on the particular fitting process of the micro-mechanical model that is employed. Different trends of changes of interfacial shear strength with respect to the fibre volume fraction were obtained depending on the fitting method used. This may be due to the complex stress-strain behaviour of the regenerated cellulose fibres which exhibit highly non-linear behaviour (with viscoelastic/viscoplastic phenomena). Moreover, the regenerated cellulose fibres are expected to show anisotropic properties. Therefore, more advanced model with improved data analysis is required. This however will make the investigated characterization method much less industrially friendly (the initial objective of this work was to validate this approach).

Nevertheless, the determined interfacial shear strength for chemically treated regenerated cellulose fibres was consistently higher than for untreated fibres. This indicates that the proposed chemical treatment of cellulosic fibres is effective, and it does improve adhesion of these fibres to the PLA matrix.

Acknowledgements

Authors affiliated with Luleå University of Technology are thankful to Hassan II Academy of Science and Technology, the Moroccan National Centre for Scientific and Technical Research, the Swedish Research Council (ref. nr. 2009-6433), and EXCEL project (funded by local government Norrbotten, SWEDEN) for their financial supports.

Emma Lindgren, MSc student at Luleå University of Technology (2015), is acknowledged for help with preparation and characterization of composites.

References

[1] Faruk O, Bledzki AK, Fink H-P and Sain M 2012 Biocomposites reinforced with natural fibers: 2000–2010 *Prog Polym Sci* **37** 1552
[2] Shah DU 2013 Developing plant fibre composites for structural applications by optimising composite parameters: a critical review *J Mater Sci* **48** 6083
[3] Belgacem MN and Gandini A 2005 The surface modification of cellulose fibres for use as reinforcing elements in composite materials *Composite Interfaces* **12** 41
[4] Qian H, Greenhalgh ES, Shaffer MS and Bismarck A 2010 Carbon nanotube-based hierarchical composites: a review *J Mater Chem* **20** 4751
[5] Lee K-Y, Ho KKC, Schlufter K and Bismarck A 2012 Hierarchical composites reinforced with robust short sisal fibre preforms utilising bacterial cellulose as binder, *Composites Sci Technol* **72** 1479
[6] Thomason JL 2002 Interfacial strength in thermoplastic composites - at last an industry friendly measurement method? Composites: Part A 33 pp 1283-1288
[7] Bowyer WH and BaderMG 1972 On the reinforcement of thermoplastics by imper-fectly aligned discontinuous fibres *J Mater Sci* **7** 1315
[8] Bader MG and Bowyer WH 1973 An improved method of production for high strength fibre-reinforced thermoplastics *Composites* **4** 150
[9] Kelly A, Tyson WR, 1965 Tensile properties of fibre-reinforced metals *J Mech Phys Solids* **13** 329
[10] Lindgren E 2015 Development and Verification of Indirect Test Method for Characterisation of

Fibre/Matrix Adhesion in Regenerated Cellulose Fibre Based Composite (Luleå: Luleå University of Technology, Thesis Master of Science in Materials Engineering), p 56
[11] Hajlane A, Kaddami H, Joffe R and Wallström L 2013 Design and characterization of cellulose fibers with hierarchical structure for polymer reinforcement *Cellulose* **20** 2765
[12] Hajlane A, Kaddami H, Joffe R 2016 A green route for modification of regenerated cellulose fibres by cellulose nano-crystals *Cellulose* (submitted, currently under review)
[13] Miettinen A, Ojala A, Wikström L, Joffe R, Madsen B, Nättinen K and Kataja M 2015 Non-destructive automatic determination of aspect ratio and cross-sectional properties of fibres *Composites Part A: Applied Science and Manufacturing* **77** 188
[14] Krenchel H 1964 Fibre reinforcement, *dr.techn.thesis* (Copenhagen)
[15] Nordström Y, Joffe R and Sjöholm E 2013 Mechanical characterization and application of Weibull statistics to the strength of softwood lignin-based carbon fibers *Journal of Applied Polymer Science* **130** 3689
[16] Joffe R, Andersons J and Sparniņš E 2009 Applicability of Weibull strength distribution for cellulose fibers with highly non-linear behaviour *Proc. 17th Int. Conf. on Composite Materials (Edinburgh, UK)* p 10
[17] Pupure L, Doroudgarian N and Joffe R 2014 Moisture uptake and resulting mechanical response of biobased composites. I. constituents", *Polymer Composites* **36** 1150
[18] Ganster J and Fink H-P 2011 Man-Made Cellulose Short Fiber Reinforced Oil and Bio-Based Thermoplastics *Cellulose Fibers: Bio- and Nano-Polymer Composites*, ed S Kalia, B S Kaith and I Kaur (Berlin Heidelberg: Springer Verlag) chapter 18 pp 479-506
[19] Modniks J, E. Poriķe, Andersons J and Joffe R 2012 Evaluation of the apparent interfacial shear strength in short-flax-fiber/PP composites *Mechanics of Composite Materials* **48** 571
[20] Andersons J, Modniks J, Joffe R, Madsen B and Nättinen K 2016 Apparent interfacial shear strength of short-flax-fiber/starch acetate composites *International Journal of Adhesion & Adhesives* **64** 78
[21] Graupner N, Fischer H, Gerhard Z and Müssig J, 2014 Improvement and Analysis of Fibre/Matrix Adhesion of Regenerated Cellulose Fibre Reinforced PP-, MAPP- and PLA-composites by the Use of Eucalyptus Globulus Lignin *Composites: Part B* **66** 117
[22] Le Duigou A, Davies P and Baley C 2010 Interfacial Bonding of Flax Fibre/Poly(L-lactide) Bio-composites *Composites Science and Technology* **70** 231
[23] Czigány T, Morlin B and Mezey Z 2007 Interfacial Adhesion in Fully and Partially Biodegradable Polymer Composites Examined with Microdroplet Test and Acoustic Emission *Composite Interfaces* **14** 869